

# ***Loss of chaos in combustion noise as a precursor of impending combustion instability***

**Vineeth Nair<sup>1</sup>, Gireehkumaran Thampi<sup>1</sup>, Sulochana Karuppusamy<sup>2</sup>, Saravanan Gopalan<sup>2</sup> and R. I. Sujith<sup>1,\*</sup>**

<sup>1</sup>National Centre for Combustion Research and Development, Department of Aerospace Engineering, Indian Institute of Technology Madras, Chennai – 36, India

<sup>2</sup>Central Electronics Centre, Department of Electrical Engineering, Indian Institute of Technology Madras, Chennai – 36, India

(Submission date: April 24, 2013; Revised Submission date: July 24, 2013; Accepted date: July 26, 2013)

## **ABSTRACT**

Combustion noise has been traditionally thought of as stochastic fluctuations present in the background of the dynamics in combustors amongst the flow, heat release and the chamber acoustics. Through a series of determinism tests, we show that these aperiodic fluctuations are in fact chaotic of moderately high dimensions ( $d_0 \cong 8-10$ ). These chaotic fluctuations then transition to high amplitude combustion instability when the operating conditions are varied towards leaner equivalence ratios. Precursors to such a transition from chaos to dynamics dominated by periodic oscillations are of interest to designers and operators of combustors in estimating the boundaries of operability. We introduce a test for chaos, known as 0–1 test for chaos in the literature, as a measure of the proximity of the combustor to an impending instability. The measure is robust and shows a smooth transition for variation in flow conditions towards instability enabling thresholds to be set for operational boundaries.

## **NOMENCLATURE**

$Re$	– flow Reynolds number
$\phi$	– equivalence ratio
$\dot{m}$	– mass flow rate
$D_1$	– characteristic dimension for the computations of Reynolds number
$D_0$	– diameter of the burner
$p(t)$	– unsteady pressure measurement
$\mu$	– dynamic viscosity

---

\*Corresponding author: sujith@iitm.ac.in

Dr. Mahesh Panchagnula served as the sole independent editor for this paper

$T$	– dominant time period during combustion instability
$\tau_{opt}$	– optimum time delay for embedding
$I$	– average mutual information
$p_i$	– point in phase space at time instant $t_i$
$d$	– embedding dimension
$d_0$	– optimum embedding dimension
$n(i, d)$	– index of the nearest neighbor
$a(i, d), E(d), E_1(d)$	– measures used to compute optimum embedding dimension
$E^*(d), E_2(d)$	– measures used to check for determinism in Cao's method
$N$	– length of the time signal
$H$	– translation horizon
$V_l$	– resultant of vectors through a hypercube
$n_j$	– number of vectors in the hypercube of index $j$
$\Lambda$	– a measure of determinism
$c_{d_0}$	– a constant involved in the computation of $\Lambda$
$q_c, r_c$	– translation variables
$\Gamma$	– gamma function
$c$	– a random variable
$M_c$	– mean square displacement
$n_{cut}$	– threshold value in the computation of $M_c$
$D_c$	– modified mean square displacement
$\xi$	– vector of time steps
$\Delta$	– vector of mean square displacements
$K_c$	– correlation of $\xi$ and $\Delta$
$K$	– median of $K_c$

## 1. INTRODUCTION

A large class of systems exists for which transition to instability is associated with the generation of well-defined oscillatory behaviour from a background of seemingly noisy signals. More often than not, such oscillations are unwanted and lead to a decreased performance and reduced lifetime of such systems.

The occurrence of such instabilities in combustors remains a challenging problem to the industry as they may be driven by a variety of flow and combustion processes which are usually coupled with one or more of the acoustic modes of the combustor [1]. Since only a small fraction of the available energy from combustion is sufficient to drive such instabilities and the corresponding attenuation in the combustion chambers is weak, large amplitude pressure oscillations are easily established in these systems resulting in performance losses, reduced operational range and structural degradation due to increased heat transfer [2, 3]. There is hence a need for reliable and robust warning signals that presage impending combustion instability.

The methodologies available in the literature to prevent large-amplitude oscillations in combustors mostly focus on suppression of an incipient instability, i.e., an instability that has already begun. The operational parameters are modified based on a feedback signal acquired from the combustor, in order to suppress the incipient instability. At

other times, modifications are made at the design stage based on operational experience as a passive control strategy. Poinot *et al.* [4] proposed a technique for the active monitoring of combustion instability through modulations of the pressure in the fuel line to suppress instabilities. This requires external actuators and/or modification of combustor configuration and knowledge of frequency response for an arbitrary input which limits its applicability to fielded systems. Further, the detection and control strategy requires the system to reach instability before control can take over. Hence, it would be more desirable to look for early warning signals to an impending instability – through active monitoring – so that instability is avoided in combustors altogether.

Hobson *et al.* [5] analyzed combustor stability in terms of the bandwidth of combustor casing vibration and dynamic pressure measurements in combustion chambers. They observed that bandwidth which is indicative of the damping decreases towards zero as the combustors approach their stability limits. However, the presence of noise in the combustion chamber could make the technique untenable in practice as it relies on a frequency domain analysis. Johnson *et al.* [6] presented a technique to determine the stability margin using exhaust flow and fuel injection rate modulation. The technique is again limited in its scope as its applicability to practical combustors is restricted by the need for acoustic drivers and pulsed fuel injectors.

Lieuwen [7] used the autocorrelation of the acquired signal to characterize the damping of the system and tracked the stability margin as the operating parameter value at which the damping goes to zero. This method again has the disadvantage that the dynamics of the system prior to onset cannot adequately be described using linear data processing techniques. The method, for instance, may not be effective for combustors exhibiting pulsed instabilities or a noise-induced transition to instability. Also, the presence of multiple frequencies often seen in the frequency spectrum at the onset makes the estimation of damping unclear.

The current solution adopted by combustion designers is thus to incorporate sufficient stability margin into the design to prevent instabilities from occurring even in the worst possible scenario. Setting such conservative estimates on operational regimes leads to increased levels of NO<sub>x</sub> emissions making it more difficult to meet the demanding emission norms. It is desirable to have measures that predict the instability well before it happens because after the onset it may often be too late to take adequate control action to save the combustor from wear and tear or fatigue failure. There is thus a need for precursors to an impending instability so that appropriate stability margins may be devised to prevent the combustors from entering a regime of instability. Also, in order that these early warning signals are sensitive to operating conditions, such as ambient temperature or fuel composition, online stability monitoring seems like the optimal solution as a prevention methodology.

There are studies where precursors to nonlinear instabilities are identified by forcing the system with broadband noise [8, 9]. When the operating conditions are sufficiently close to the onset, the noise gets selectively amplified at the instability frequencies. The width of the peak corresponding to the dominant frequency in the spectrum is then used as an indicator of the proximity of the system to instability [8]. Further, it has also been shown that there is a reduction in the width of the hysteresis zone for triggered

instabilities when the noise levels are increased [9]. However, as noted earlier, an analysis in the frequency domain is often insufficient and external stochastic forcing can modify the dynamics of the system itself resulting in detrimental noise-induced transitions [10].

Traditionally, unsteady measurements acquired from combustors are treated as signals modulated by random noise perturbations. The irregular low amplitude pressure fluctuations and flow turbulence are often treated as stochastic background to the dynamics and are either averaged out or neglected [11–16]. Linear stability of the system is then estimated from the averaged equations. Despite the progresses made in the understanding of combustion instabilities, considerable difficulties still exist in the prediction of the boundaries of stable operation, i.e., the stability margins [17]. This difficulty could be a consequence of the traditional ‘signal plus noise’ paradigm assumed in the analysis of such oscillations. Hence, it behooves researchers in the field to estimate the levels of determinism in the measurements made at operating conditions classified as combustion noise in the literature.

A good understanding of how the dynamics of the combustors transition from low amplitude, combustion amplified, turbulence noise to high amplitude, periodic instabilities is required in order that appropriate precursors are found that presage the onset of instabilities. Through a systematic variation of operating conditions in a bluff-body and backward-facing step combustors, Chakravarthy *et al.* [18, 19] identified that a ‘lock-on’ mechanism between the vortex shedding and duct acoustics was responsible for the transition from stable to unstable operation. Whereas the non-lock-on regime is characterized by low-amplitude broadband noise generation, the onset of lock-on is characterized by the excitation of high-amplitude, tonal oscillations. In another experimental study where the equivalence ratio was varied [20], the transition of the dynamics was reported to vary from stochastic fluctuations to periodic oscillations through low dimensional chaotic oscillations.

The principal aim of the current study is to understand whether the measured signals during regimes of combustion noise shows signs of determinism. The presence of determinism allows for measures to be defined that can predict the onset of combustion instability. Techniques from nonlinear time series analysis have already been applied to predict lean blowout in gas turbines [21]. In a similar vein, the present study tries to identify precursors to impending combustion instability, through active monitoring, allowing for quick and efficient prevention of oscillations and thereby extend the boundaries of operability of combustors.

## 2. EXPERIMENTAL CONFIGURATION

The determinism in combustion noise data was assessed on the unsteady pressure signals acquired from two combustors – a swirl-stabilized backward facing step combustor and a bluff-body stabilized backward facing step combustor – operating at high Reynolds numbers. The schematic of the setups is shown in Fig. 1. It comprises a plenum chamber, a shaft of diameter 10 mm housed in a burner of 40 mm diameter that supports the vane swirler or bluff-body and a combustion chamber of length 300 mm with two extension ducts of lengths 300 mm and 100 mm. The swirler, has 8 blades at

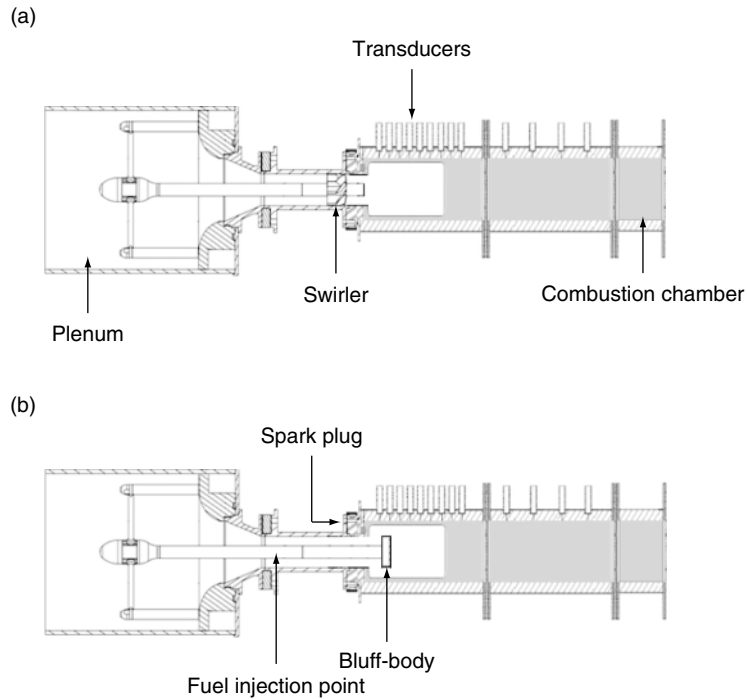


**Figure 1:** The combustors used in the current study. (a) A swirl-stabilized backward facing step combustor. (b) A bluff-body stabilized backward facing step combustor. The fuel (LPG) is injected through four radial holes in the central shaft. The fuel injection location was 100 mm upstream from the swirler and 160 mm upstream from the bluff-body. The length of the combustion chamber is 700 mm with three extension ducts of lengths 300 mm, 300 mm and 100 mm respectively. The location of the bluff-body is 50 mm from the rearward-facing step. The design of combustor was adapted from [23].

an angle of  $45^\circ$  with a swirl number of 0.7, and a center-body for flame stabilization which was placed so that it grazes the edge of the burner. For experiments using the bluff-body, a circular disk of diameter 47 mm and thickness 10 mm was used. The bluff-body was placed at a distance of 50 mm from the backward facing step using a traverse of least count 1 mm. The burner was provided with a flashback arrestor which was a circular disk of thickness 2 mm with 300 holes of diameter 1.7 mm located 30 mm downstream of the fuel-injection location. The combustion chamber has a square geometry of cross-section  $90 \times 90 \text{ mm}^2$  which provided a sudden expansion from the burner exit. The fuel-air mixture was ignited using a spark plug with a step-up transformer which was mounted in the dump plane. Fuel was delivered using the central shaft through four radial injection holes of diameter 1.7 mm.

To control the flow rates of air and fuel, mass flow controllers (Alicat Scientific, MCR Series) with digital logging and monitoring capabilities were used with an uncertainty of  $\pm (0.8\% \text{ of reading} + 0.2\% \text{ of full scale})$ . Unsteady pressure measurements were made using a piezoelectric transducer (sensitivity  $72.5 \text{ mV/kPa}$ , resolution  $0.48 \text{ Pa}$  and uncertainty of  $\pm 0.64\%$ ) mounted on specially made pressure ports flush-mounted on the combustor walls and placed  $90 \text{ mm}$  from the rearward facing step. To ensure near-adiabatic boundary conditions, wall cooling was not provided and the operation of the combustor was restricted to short durations. A Teflon adapter was used to protect the transducer from excess heating and the mount was designed to ensure integrity in the measured signals. A 16-bit A-D conversion card (NI-643) with an input voltage range of  $\pm 5 \text{ V}$  and a resolution of  $\pm 0.15 \text{ mV}$  was used to acquire the signals from the transducers.

The ambient temperature was measured to be  $(27 \pm 1)^\circ\text{C}$  using a dry bulb thermometer and the relative humidity was measured to be  $(85 \pm 1)\%$  on a hygrometer for all the experiments. The fuel used was LPG (60%  $\text{C}_4\text{H}_{10}$  and 40%  $\text{C}_3\text{H}_8$ ). The flow Reynolds number was calculated using the formula  $Re = 4\dot{m}D_1/\pi\mu D_0^2$ , where  $\dot{m}$  is the mass flow rate of the fuel-air mixture,  $D_1$  is the characteristic dimension (diameter of the swirler/bluff-body),  $\mu$  is the dynamic viscosity of the fuel-air at the experiment conditions and  $D_0$  is burner diameter. Viscosity corrections were made for Reynolds number calculations for changes in the fuel-air ratio, using the formula of viscosity for binary mixtures given in [22].

The decay rates of the combustion chamber were measured multiple times for both the combustors prior to the experiments to ensure that the ambient conditions and the acoustic damping of the system did not change between the experiments. To obtain these decay rates, the combustors were forced with a loudspeaker placed at the exit at the cold natural acoustic fundamental frequency ( $133 \text{ Hz}$  for the swirl-stabilized combustor and  $135 \text{ Hz}$  for the bluff-body stabilized combustor). Then the exponential fall-off of the signal was measured when the forcing was switched off. The decay rate was then obtained as the slope of a semi-log plot of the amplitude decay with time. These decay rates had an average value of  $-37\text{s}^{-1}$  with a variation of less than 3% including the configuration change from swirler to bluff-body.

Unsteady pressure measurements were made in a sequential manner for increases in flow Reynolds numbers from stable combustion to combustion instability. The time series was acquired at  $10 \text{ kHz}$  for a duration of  $3\text{s}$ .

### 3. PHASE SPACE RECONSTRUCTION

The amount of experimental data available at the disposal of an experimental researcher is often just a few variables and in extreme cases just one. Recent developments in the field of nonlinear time series analysis [24] can provide valuable insights into the system dynamics which can then yield a better understanding of the underlying mechanisms of transitions useful in eventual modelling. The application of nonlinear time series analysis to signals acquired from thermoacoustic systems has been demonstrated by [25].

### 3.1. Methodology

The dynamics of a combustor at different operating conditions can be visualized by reconstructing the mathematical phase space of evolution of the time series data of unsteady pressure measurements acquired at those conditions. In such a reconstructed phase space [26], limit cycle oscillations would correspond to a closed loop around a fixed point. Such a reconstruction, also known as delay-embedding, entails converting the measured time series into a set of delay vectors each of which has a one-to-one correspondence with one of the dynamic variables involved in the combustor dynamics. That is, we construct the vectors  $[p(t), p(t + \tau), p(t + 2\tau), \dots, p(t + d - 1)\tau]$  from the measured pressure data  $p(t)$  such that these vectors in combination provide us with maximum information on the combustor dynamics. The elements of these vectors are the coordinates in the  $d$ -dimensional phase space of evolution of the time signal. For instance,  $\mathbf{p}_i(d) = [p(t_i), p(t_i + \tau), p(t_i + 2\tau), \dots, p(t_i + d - 1)\tau]$  is the point in the  $d$ -dimensional phase space at time instant  $t_i$ . To accomplish an appropriate reconstruction, we need to obtain the optimum time lag ( $\tau_{opt}$ ) amongst the delay vectors and the least embedding dimension ( $d$ ) for the phase space composed of these delay vectors such that the dynamics is faithfully captured.

The optimum delay  $\tau_{opt}$  may be estimated as that value of  $\tau$  for which the average mutual information [24] between the delay vectors reaches its first minimum. The average mutual information of a signal  $p(t)$  is given by the expression:

$$I(\tau) = \sum_{i=1}^N P(p(t), p(t + \tau)) \log_2 \left[ \frac{P(p(t), p(t + \tau))}{P(p(t))P(p(t + \tau))} \right] \quad (1)$$

where,  $P(S)$  represents the probability of the event  $S$

To compute the average mutual information for various time lags  $\tau$ , we first normalize the time signal  $p(t)$  to lie between 0 and 1 and then sort the data in bins. The probability distributions  $p(t)$  and  $p(t + \tau)$  are then obtained by normalizing the histograms on these bins. Similarly, the joint probability distribution  $P(p(t), p(t + \tau))$  is obtained by normalizing a two dimensional histogram obtained on a two dimensional bin in  $p(t)$  and  $p(t + \tau)$ .

Average mutual information, which is a function of the time distance between the data points of a time series, is an indicator of the amount of information shared by two sets of data. The location of the minimum would, therefore, correspond to a set of vectors that would provide more information about the system than either of them in isolation.

To obtain a suitable dimension  $d$  in which the attractor dynamics unfold, we use the technique developed by Cao [27]. This is an optimized version of the False Nearest Neighbors method [24] wherein one tracks the number of false neighbours to each point in the phase space as the embedding dimension is progressively increased. A false neighbour to a point in phase space is one that moves away from it once the embedding dimension is increased. Mathematically, once the optimum time lag has been obtained, we can construct a measure  $a(i, d)$  of the form:

$$a(i, d) = \frac{\|p_i(d+1) - p_{n(i,d)}(d+1)\|}{\|p_i(d) - p_{n(i,d)}(d)\|} \quad (2)$$

where  $i = 1, 2, \dots, (N-d\tau)$  and  $n(i, d)$  is the index of the nearest neighbouring point in phase space to the point  $p_i$ .  $\|\dots\|$  represents the Euclidean distance between two points. The dependency on the index  $i$  is removed by taking the average  $a(i, d)$  obtained at different values of  $i$  as:

$$E(d) = \frac{1}{N-d\tau_{opt}} \sum_{i=1}^{N-d\tau_{opt}} a(i, d) \quad (3)$$

Here,  $E(d)$  is a function only of the dimension  $d$  and the optimum time lag  $\tau_{opt}$ . The variation of  $E(d)$  on increasing the dimension from  $d$  to  $d+1$  is determined by defining  $E_1(d)$  as:

$$E_1(d) = \frac{E(d+1)}{E(d)} \quad (4)$$

If  $E_1(d)$  stops changing when the value of  $d$  is greater than  $d_0$ , then  $d_0+1$  is chosen as the minimum embedding dimension for the time series. Since the acquired time signal is limited, it is often difficult to distinguish a stochastic signal from a deterministic signal merely by observing the variation of  $E_1(d)$  for various values of  $d$ . Whereas  $E_1(d)$  saturates beyond a value of  $d$  for a deterministic signal, it always increases with increasing  $d$  for random signals. To clearly distinguish deterministic signals from stochastic signals, we define an additional measure  $E_2(d)$  from the time series  $p(t)$  as:

$$E_2(d) = \frac{E^*(d+1)}{E^*(d)} \quad (5)$$

where

$$E^*(d) = \frac{1}{N-d\tau_{opt}} \sum_{i=1}^{N-d\tau_{opt}} |p(i+d\tau_{opt}) - p(n(i,d)+d\tau_{opt})| \quad (6)$$

Since future values are independent of past values for random signals,  $E_2(d)$  equals 1 for all values of  $d$  (independent of  $d$ ) [27]. For deterministic signals on the other hand,  $E_2(d)$  is dependent on  $d$ , because of which there must exist some values of  $d$  for which  $E_2(d)$  is not equal to 1.

### 3.2. Delay embedding of combustion noise

The technique of phase space reconstruction detailed above was applied to the unsteady pressure signals acquired from the two combustors. The signals are varying in amplitudes and appear rather aperiodic (Fig 2 a, d). The average mutual information for the two sets of data have their first minimum at  $\tau_{opt} = 1.2$  ms and  $\tau_{opt} = 1.1$  ms

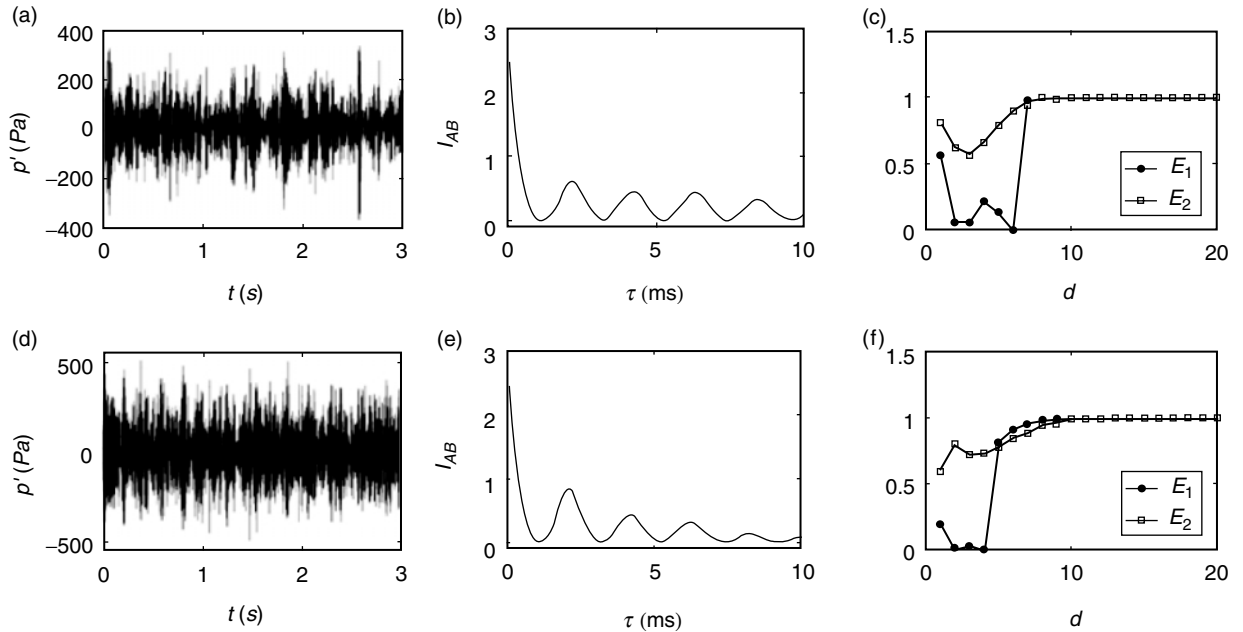


**Figure 2:** Phase space reconstruction of combustion noise data from (a) combustor with a swirl-stabilized flame ( $\phi = 1.0$ ,  $Re = 1.6 \times 10^4$ ), and (d) combustor with a bluff-body stabilized flame ( $\phi = 1.1$ ,  $Re = 1.8 \times 10^4$ ). The average mutual information for the two signals are shown in (b) and (e) respectively. The optimal delay are  $\tau_{opt} = 1.2$  ms and  $\tau_{opt} = 1.1$  ms. Results on applying Cao's method of obtaining the embedding dimension are shown in (c) and (f). The plot of  $E_1(d)$  saturates around  $d = 7$  for the data from swirl-stabilized combustor and  $d = 8$  for the data from bluff-body stabilized combustor. Also, the values of  $E_2(d)$  do not equal 1 for all values of  $d$ . This indicates that combustion noise is deterministic and possibly chaotic with moderately high dimensions ( $d_0 \approx 8-10$ ).

respectively. These values correspond approximately to  $T/4$  where  $T$  is the time period of oscillation at combustion instability. This time period was discerned from the FFT of the pressure signal at combustion instability. The delay vector  $p(t_i + \tau_{opt})$  can thus alternately be seen to be related to the acoustic velocity in a one-to-one fashion since the acoustic pressure and velocity differ in phase by approximately  $90^\circ$  for a standing wave pattern in the duct. The small deviations from  $90^\circ$  are due to damping.

The least embedding dimension for the two combustors can be taken to be  $d_0 = 8$  as the measure  $E$  does not vary significantly after  $d = 7$ . Also, the value of the measure  $E_2(d)$  is not equal to 1 for all values of  $d$ . Hence, we see that combustion noise is deterministic and possibly chaotic with a moderately high dimensional attractor. Although, Cao's method to determine the least embedding dimension provides us with

information as to whether the signal is deterministic or not, additional tests for determinism are often performed to confirm the finding. One of such methods is described below.

#### 4. TESTS FOR DETERMINISM

##### 4.1. The local flow test for determinism

The local flow test for determinism is a discrete adaptation [28] of a technique devised by Kaplan and Glass [29] for continuous dynamical systems. After delay-embedding the time series, one selects points in the phase space that are close to each other. These points are then evolved in time for a short duration known as the translation horizon. Points in the phase space that are close to each other tend to move in the same direction for deterministic signals and in random directions for stochastic signals. Hence, for a given translation horizon, we construct vectors that connect the initial and final points, which are then normalized and averaged. These averaged vectors would then be larger for deterministic signals. The process is then repeated for various translation horizons. For deterministic signals, although the deterministic structure is preserved for short horizons, it is lost once the translation horizon is made too large. Hence, the average vector lengths will be small once the translation horizon is made large.

To construct a measure of determinism, we first cover the phase space with a grid of non-overlapping hypercubes (cubes in  $d$  dimensions). The number of points in each cube is  $n_j$  with time indices  $t_{j,1}, t_{j,2}, \dots, t_{j,n_j}$ . If  $H$  is the translation horizon, the change in state from time  $t_{j,k}$  to  $t_{j,k} + H$  for each of the  $n_j$  points in the cube  $j$  is given by:

$$\Delta \mathbf{p}_{j,k} = \mathbf{p}(t_{j,k} + H) - \mathbf{p}(t_{j,k}) \quad (7)$$

where  $k = 1, 2, \dots, n_j$ . Note that here we have explicitly written out the index in terms of time to distinguish different points within the same hypercube. Points near the edge of a cloud of points will have a directional bias towards the middle of the cloud [28]. To correct for this,  $\Delta \mathbf{p}_{i,k}$  is mapped onto a sine function as:

$$\Delta \mathbf{p}_{j,k} = \begin{bmatrix} \sin\left(2\pi \frac{p(t_{j,k} + H) - p(t_{j,k})}{\lambda}\right), \sin\left(2\pi \frac{p(t_{j,k} + H + \tau) - p(t_{j,k} + \tau)}{\lambda}\right), \dots, \\ \sin\left(2\pi \frac{p(t_{j,k} + H + (d-1)\tau) - p(t_{j,k} + (d-1)\tau)}{\lambda}\right) \end{bmatrix}$$

where  $\lambda$  is the characteristic length of the embedded attractor in phase space. Summing up all vectors through hypercube of index  $j$ , we obtain the resultant vector  $\mathbf{V}_j$  normalized by the number of vectors passing through the cube  $n_j$  in the following fashion:

$$\mathbf{V}_j = \frac{1}{n_j} \sum_k \frac{\Delta \mathbf{p}_{j,k}}{\|\Delta \mathbf{p}_{j,k}\|} \quad (8)$$

We can then define a measure  $\Lambda$  that quantifies local flow in phase space by averaging over the vectors  $\mathbf{V}_j$  based on the number of vectors present in the hypercube (say,  $l$ ), as:

$$\Lambda = \left\langle \frac{V_l^2 - c_{d_0}^2 / l}{1 - c_{d_0}^2 / l} \right\rangle \quad (9)$$

Here,  $V_l$  represents the norm of  $\mathbf{V}_l$  (the replaced index in the subscript indicative of the new ordering) and  $c_E$  is a constant defined as [29]:

$$c_{d_0} = \sqrt{\frac{2}{d_0}} \frac{\Gamma\left(\frac{d_0+1}{2}\right)}{\Gamma\left(\frac{d_0}{2}\right)} \quad (10)$$

with  $\Gamma$  being the standard gamma function. The measure  $\Lambda$  retains values close to 1 for deterministic signals and has values close to 0 for stochastic signals [29].

Although  $\Lambda$  quantifies local flow, it is insensitive to whether the source is determinism or directional preference due to autocorrelations. The method of surrogate data helps to circumvent this uncertainty.

#### 4.2. Surrogate data analysis

Interpretation of results from experimentally acquired data can sometimes pose problems because filtered noise data can sometimes give the impression of chaos and low-dimensional dynamics. The technique of surrogate data analysis provides an efficient method to avoid such misinterpretations. One starts the analysis with a null hypothesis (or the default position in the absence of evidence to the contrary) that the experimental data can be described by a linear stochastic model. Surrogate data sets are generated from a measured signal such that they retain certain characteristics of the original data (such as number of data points, mean and standard deviation) while ensuring that the data is sufficiently randomized so that any deterministic structure that may be present in the original data is destroyed [30]. Techniques like the determinism tests are then applied to both the original data and the surrogate data. If the results are similar for the experimental and surrogate data sets; i.e., if the predictions of the tests are equally good or bad, then one cannot reject the null hypothesis that a linear stochastic model is sufficient to describe the experimental data.

One of the techniques of surrogate generation involves randomly shuffling the data values in the signal, without adding or subtracting data [31]. Such a random shuffling destroys any correlation originally present among the data points. This produces a random time signal that has the same mean and standard deviation as the original time series.

### 4.3. Determinism in combustion noise

Surrogate data sets were constructed from unsteady pressure measurements acquired during combustion noise with the same mean and standard deviation as the original data. Then the local flow test for determinism was applied on both the original and surrogate data sets and the results are shown in Fig. 3. Whereas the levels of determinism remain fairly high for the original data over a range of translation horizons, they remain at a low value for the surrogate data sets. The occasional spikes correspond to those values of translation horizon which are multiples of  $\tau_{opt}$  (in time steps). This happens because the delay vectors partially overlap after moving over a distance  $\tau_{opt}$  which also happens to be the optimum delay chosen for embedding. Hence, we have convincing evidence that combustion noise is deterministic. Thus, the traditional signal plus noise paradigm often implicitly assumed in models and analysis of experimental data sets [11–16] needs to be reexamined if one wishes to capture the onset of instabilities in combustors because these irregular fluctuations may contain useful information of prognostic value.

## 5. THE 0-1 TEST FOR CHAOS [32]

### 5.1. Computational procedure

The motivation behind the test is that when the combustor encounters limit cycle oscillations, the dynamics transitions from chaotic to regular. The signal  $p(t)$  is measured ensuring that the acquired value at each instant provides essentially little information about future values at stable operation. This can be done by sampling at a time interval corresponding to the minimum of the average mutual information. Typically, this would correspond to a sampling time of  $\tau_{opt} = T/4$  where  $T$  is the period of oscillations in the combustion chamber during instability. Typically, the time period of oscillations at instability is itself an unknown. However, the detector is robust for various values of sampling interval as long as the consecutive values are poorly correlated. For example, comparable results can be obtained for values of  $\tau_{opt}$  corresponding to the first zero crossing of the autocorrelation of  $p(t)$ . The time period corresponding to the dominant frequency in the FFT during stable operation of the combustor can also be utilized as a suitable measure of  $T$  to obtain the sampling time.

From the measured signal  $p(t)$  for  $t = (1, 2, \dots, N)$  and  $t_i + 1 - t_i = \tau_{opt}$ , translation variables  $q_c$  and  $r_c$  can be created as follows:

$$q_c(n) = \sum_{t=1}^n p(t) \cos(tc) \quad (11)$$

$$r_c(n) = \sum_{t=1}^n p(t) \sin(tc) \quad (12)$$

where  $c \in (\pi/5, 4\pi/5)$ . The mean square displacement of these translation variables may then be computed for different values of  $c$  as following:

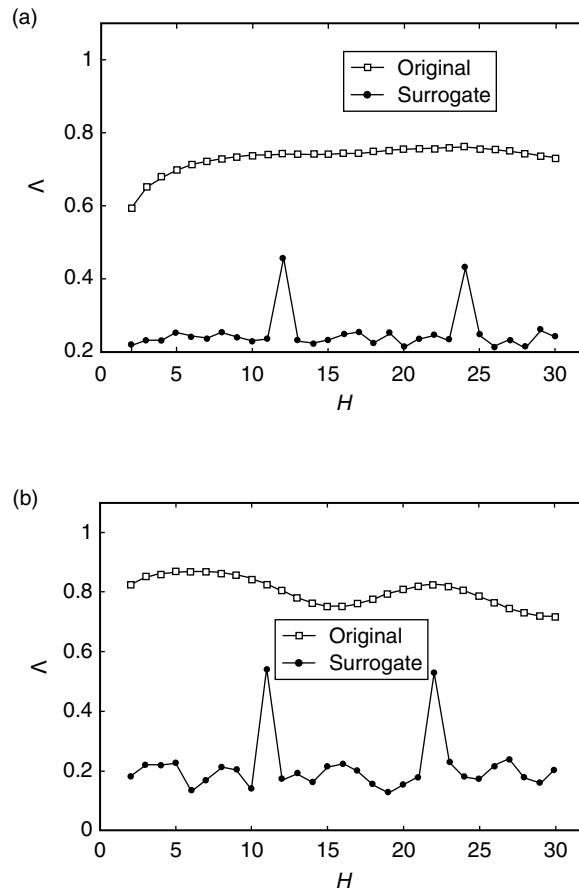


**Figure 3:** Results on applying the local flow method of determinism on the combustion noise data from (a) combustor with a swirl-stabilized flame ( $\phi = 1.0$ ,  $Re = 1.6 \times 10^4$ ,  $\tau_{opt} = 1.2$  ms), and (d) combustor with a bluff-body stabilized flame ( $\phi = 1.1$ ,  $Re = 1.8 \times 10^4$ ,  $\tau_{opt} = 1.1$  ms). Whereas the original data shows high levels of determinism, it is lost when the data values are randomly shuffled. The embedding dimension was maintained as  $d_0 = 10$  for all the data sets.  $\tau_{opt}$  for the surrogate sets was maintained the same as that for original data for the sake of comparison. The spikes in the surrogate data correspond to those values of translation horizon  $H$  that are multiples of the optimum time delay  $\tau_{opt}$  non-dimensionalized by the sampling time.

$$M_c(n) = \lim_{N \rightarrow \infty} \frac{1}{N} \sum_{t=1}^N \left( [q_c(t+n) - q_c(t)]^2 + [r_c(t+n) - r_c(t)]^2 \right) \quad (13)$$

with  $n \ll N$ . It is seen that  $n \leq n_{cut}$  where  $n_{cut} = N/10$  yields good results.

The mean square displacement is indicative of the diffusive nature of the translation variables. If the dynamics is regular, then the mean square displacement is a bounded function in time and for chaotic dynamics, it scales linearly with time.

A modified mean square displacement  $D_c$  may be defined to ensure better convergence properties but with the same asymptotic growth rate as [32]:

$$D_c(n) = M_c(n) - V_{osc}(n) \quad (14)$$

where

$$V_{osc}(c, n) = \langle p(t) \rangle^2 \frac{1 - \cos nc}{1 - \cos c} \quad (15)$$

and

$$\langle p(t) \rangle = \lim_{N \rightarrow \infty} \frac{1}{N} \sum_{t=1}^N p(t) \quad (16)$$

Hence by defining vectors  $\xi = (1, 2, \dots, n_{cut})$  and  $\Delta = (D_c(1), D_c(2), \dots, D_c(n_{cut}))$ , the correlation  $K_c$  given by:

$$K_c = \text{corr}(\xi, \Delta) \quad (17)$$

essentially allows one to distinguish between the two types of behavior possible in such systems.

To ensure robustness of the measure to outliers and spurious resonances, the median value of  $K_c$  (say  $K$ ) may be taken which is obtained for different random values of  $c$ . This value of  $K$  would lie close to 1 for chaotic signals and close to 0 for regular dynamics. If the system is inherently turbulent, the transition to instability would be associated with a decrease in the value of  $K$  from 1 to a value depending on the turbulent intensity, i.e., higher the intensity of turbulence at instability higher the departure of  $K$  from 0 at instability.

## 5.2. Prediction of impending combustion instability

The 0–1 test for chaos was applied on the pressure measurements acquired sequentially at various Reynolds numbers starting from low amplitude combustion noise to high amplitude combustion instability. The measure  $K$  remains fairly close to 1 during the initial stages which indicates that combustion noise is chaotic. The value of  $K$  gradually starts decreasing as the flow Reynolds numbers are increased, eventually reaching values close to 0 at the onset of instabilities. Since this loss of chaos happens in a smooth manner, we can use the measure  $K$  as a precursor to impending instability. By choosing a threshold value of  $K$  that corresponds to the initial stages of loss of chaos

(say, 0.9), operators get to know well in advance of an impending instability so that appropriate control action may be taken through modification of control parameters to prevent the onset. The precursor is thus an objective measure of proximity of the combustor to unstable operating regimes and is independent of the details of geometry, fuel composition and flame stabilization.

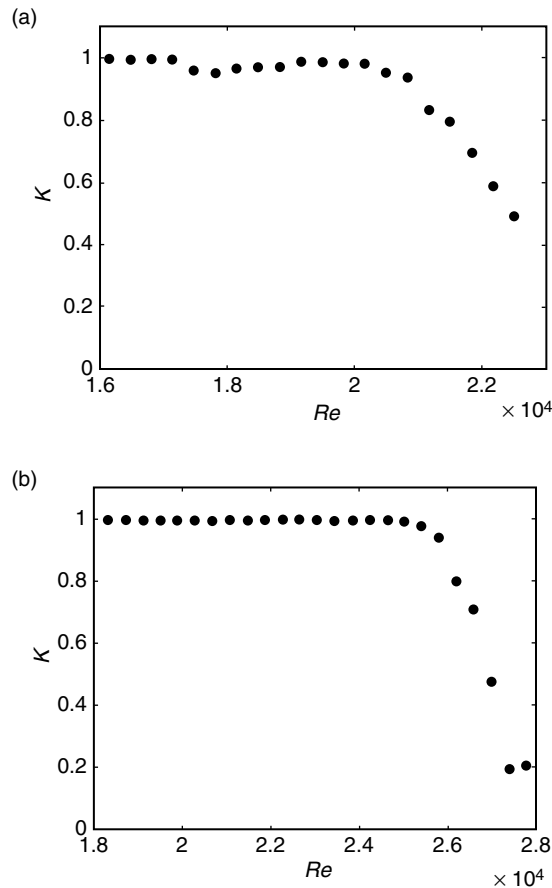


**Figure 4:** The results on applying the 0–1 test for chaos on (a) the swirl-stabilized backward facing step combustor and (b) the bluff-body stabilized backward facing step combustor for signals acquired at various Reynolds number. Whereas the values lie fairly close to 1 for chaotic combustion which is stable, departure from 1 indicates the onset of impending combustion instability which happens as the Reynolds number is increased. The results presented are for the entire 3s data which brings in some graininess due to amplitude modulations. By setting threshold at a value of say 0.9 for  $K$ , operators can be informed of an impending instability so that appropriate control measures can be taken.

We successfully devised a controller [33] that determines the proximity of combustors to instability that utilizes the 0–1 test for chaos. Although we used the entire 3s data in the analysis results presented in Figure 4, the test performs robustly even with a sampling rate as poor as 1 kHz with 500 samples of data (data acquisition for 500 ms) for an instability frequency around 250 Hz.

Since the measure falls smoothly as the operating conditions approach onset, suitable control action may be taken by modifying operational parameters to prevent high amplitude oscillations. Thus, the stability margins of practical fielded systems can safely be estimated without encountering instabilities.

## 6. CONCLUDING REMARKS

Combustion noise was shown to be deterministic by performing the Kaplan-Glass test for determinism on unsteady pressure data acquired from two different combustors operating at turbulent Reynolds numbers. The present study further identifies precursors to impending combustion instability, using the departure from chaos as an early warning signal to impending instability, thereby improving the operational boundaries of practical fielded combustors. Combustion noise is thus shown to be deterministic chaos, which is in stark contrast with the current description of the phenomenon where it is often assumed to be a stochastic background to the dynamics. This signal plus noise paradigm which involves decomposing the data into a signal and accompanying noise often overlooks the prognostic value of the irregular fluctuations that, as this study shows can forewarn an operator of impending combustion instability.

## ACKNOWLEDGEMENTS

This work was funded by the Department of Science and Technology, Government of India. The authors acknowledge the help of Mr. Gopalakrishnan and Mr. Vishnu from IIT Madras in performing the experiments.

## REFERENCES

- [1] F. E. C. Culick, Unsteady motions in combustion chambers for propulsion systems, 2006, Vol. AG-AVT-039. RTO AGARDograph.
- [2] K. R. McManus, T. Poinso, and S. M. Candel, A review of active control of combustion instabilities, *Prog. Energy Combust. Sci.*, 1993, 16, 1–29.
- [3] S. Candel, Combustion dynamics and control: Progress and challenges, *Proceedings of the Combustion Institute*, 2002, 29, 1–28.
- [4] T. Poinso, F. Lacas, J. Chambon, D. Veynante, and A. Trouve, “Apparatus for active monitoring of combustion instability”, US patent (US 5145355 A) filed on September 8, 1992.
- [5] D. E. Hobson, J. E. Fackrell, and G. Hewitt, Combustion instabilities in industrial gas turbines: Measurements on operating plant and thermoacoustic modeling, *Journal of Engineering for Gas Turbines and Power*; 2000, 122, 420–428.

- [6] C. E. Johnson, Y. Neumeier, T. C. Lieuwen, and B. T. Zinn, Experimental Determination of the Stability Margin of a Combustor Using Exhaust Flow and Fuel Injection Rate Modulation, *Proceedings of the Combustion Institute*, 2000, 28, 757–763.
- [7] T. Lieuwen, Online Combustor Stability Margin Assessment Using Dynamic Pressure Data, *J. Eng. Gas Turbines Power*, 2005, 127, 478–482.
- [8] K. Wiesenfeld, Noisy precursors of nonlinear instabilities, *Journal of Statistical Physics*, 1985, 38, 1071–1097.
- [9] E. Surovyatkina, Prebifurcation noise amplification and noise-dependent hysteresis as indicators of bifurcations in nonlinear geophysical systems, *Nonlinear processes in geophysics*, 2005, 12, 25–29.
- [10] V. Jegadeesan and R.I. Sujith, Experimental investigation of noise induced triggering in thermoacoustic systems, *Proceedings of the Combustion Institute*, 2013, 34, 3175–3183.
- [11] P. Clavin, J. S. Kim, and F. A. Williams, Turbulence-induced noise effects on high-frequency combustion instabilities. *Combust. Sci. Tech.*, 1994, 96, 61–85.
- [12] V. S. Burnley, and F. E. C. Culick, Influence of random excitations on acoustic instabilities in combustion chambers, *AIAA J.*, 2000, 38, 1403–1410.
- [13] T. C. Lieuwen, Phase Drift Characteristics of Self Excited, Combustion Driven Oscillations, *J. Sound Vib.*, 2001, 242, 893–905.
- [14] T. C. Lieuwen, Experimental investigation of limit-cycle oscillations in an unstable gas turbine combustor, *J. Prop. Power*, 2002, 18, 61–67.
- [15] T. C. Lieuwen, Statistical characteristics of pressure oscillations in a premixed combustor. *J. Sound Vib.*, 2003, 260, 3–17.
- [16] T. Lieuwen, and A. Banaszuk, Background noise effects on combustor stability. *J. Prop. Power*, 2005, 21, 25–31.
- [17] B. T. Zinn., and T. C. Lieuwen, (Eds. T. C. Lieuwen, and V. Yang) Combustion instabilities in gas turbine engines: Operational experience, fundamental mechanisms, and modeling, Chapter 1: Combustion instabilities: Basic concepts, AIAA Inc., 2005, Vol. 210.
- [18] S. R. Chakravarthy, R. Sivakumar, and O. J. Shreenivasan, Vortex-acoustic lock-on in bluff-body and backward-facing step combustors, *Sadhana*, 2007a, 32, 145–154.
- [19] S. R. Chakravarthy, O. J. Shreenivasan, B. Boehm, A. Dreizler, and J. Janicka, Experimental characterization of onset of acoustic instability in a nonpremixed half-dump combustor, *J. Acoust. Soc. Am.*, 2007b, 122, 120–127.
- [20] H. Gotoda, H. Nikimoto, T. Miyano, and S. Tachibana, Dynamic properties of combustion instability in a lean premixed gas-turbine combustor, *Chaos*, 2011, 21, 013124:1–11.

- [21] A. Mukhopashyay, R. R. Chaudhari, T. Paul, S. Sen and A. Ray, Lean Blow-Out Prediction in Gas Turbine Combustors Using Symbolic Time Series Analysis, *Journal of Propulsion and Power*, 2013, DOI: 10.2514/1.B34711.
- [22] C. R. Wilke, A viscosity equation for gas mixtures, *The Journal of Chemical Physics*, 1950, 18, 517–519.
- [23] T. Komarek, and W. Polifke, Impact of swirl fluctuations on the flame response of a perfectly premixed swirl burner, *J. Eng. Gas Turb. Power*, 2010, 132, 061503:1–7.
- [24] H. D. I. Abarbanel, R. Brown, J. J. Sidorowich, and L. Tsimring, The analysis of observed chaotic data in physical systems, *Reviews of Modern Physics*, 1993, 65, 1331–1392.
- [25] L. Kabiraj and R. I. Sujith, Nonlinear self-excited thermoacoustic oscillations: intermittency and flame blowout, *J. Fluid Mech.*, 2012, 713, 376–397.
- [26] F. Takens, Detecting strange attractors in turbulence. In *Dynamical Systems and Turbulence*, Warwick 1980 (eds. R. David & L.-S. Young). *Lecture Notes in Mathematics*, 898, pp. 366–381. Springer.
- [27] L. Cao, Practical method for determining the minimum embedding dimension of a scalar time series, *Physica D*, 1997, 110, 43–50.
- [28] D. T. Kaplan, Evaluating deterministic structure in maps deduced from discrete-time measurements, *Int. J. Bifurcations and Chaos*, 1993, 3, 617–623.
- [29] D. T. Kaplan, and L. Glass, Direct test for determinism in a time series, *Phys. Rev. Lett.*, 1992, 68, 427–430.
- [30] J. Theiler, S. Eubank, A. Longtin, B. Galdrikian, and J. D. Farmer, Testing for nonlinearity in time series: the method of surrogate data, *Physica D*, 1992, 58, 77–94.
- [31] B. J. West, *Where medicine went wrong: Rediscovering the path to complexity*, 2006, World Scientific, p. 55.
- [32] G. A. Gottwald, and I. Melbourne, A new test for chaos in deterministic systems, *Proc. R. Soc. Lond. A*, 2004, 460, 603–611.
- [33] V. Nair, G. Thampi, K. Sulochana, G. Saravanan, and R. I. Sujith, “System and method for predetermining the onset of impending oscillatory instabilities in practical devices”, Provisional patent, filed Oct. 1 2012.